MicroRNA-122 Regulates Polyploidization in the Murine Liver

Shu-hao Hsu*, Evan R. Delgado*, P. Anthony Otero, Kun-yu Teng, Huban Kutay, Kolin M. Meehan, Justin B. Moroney, Jappmann K. Monga, Nicholas J. Hand, Joshua R. Friedman, Kalpana Ghoshal and Andrew W. Duncan (* These authors contributed equally to the work)

Hepatology 2016

Supporting Information

Supporting Materials and Methods

Supporting Figures

Supporting Tables (*included elsewhere as a single spreadsheet with multiple tabs*)

Supporting Information

Supporting Materials and Methods

Histology. *Mir122*-deficient, control and WT C57BL/6 livers were fixed in 4% paraformaldehyde (PFA), embedded in optimal cutting temperature (OCT) compound (Sakura Finetek, Torrance, CA) and cryosectioned at a thickness of 4 µm. Additionally, *Mir122*-deficient/control, WT C57BL/6 and *Dicer1*-LKO/control livers were fixed in neutral buffered formalin, embedded in paraffin and sectioned at a thickness of 4 µm. Frozen liver sections were stained according to manufactures' instructions with Phalloidin Alexa Fluor 488 (Life Technologies) or primary antibodies for PCNA and p21 (both from Santa Cruz) followed by species-specific secondary antibodies Goat anti-Mouse/Alexa Fluor 488 and Goat anti-Rabbit/ Alexa Fluor 488 from Life Technologies. The terminal deoxynucleotidyl transferase-mediated dUTP nick-end labeling (TUNEL) assay was performed as described (Roche, Indianapolis, IN) and positive cells were visualized with Streptavidin/Alexa Fluor 488 (Life Technologies). All sections were counterstained with Hoechst 33342 (Life Technologies) and mounted with Fluoromount-G (SouthernBiotech, Birmingham, AL). Paraffin sections were stained sequentially with primary and secondary antibodies following citric acid-based antigen retrieval (Vector, Burlingame, CA): anti-β-catenin (Santa Cruz) or anti-Ki-67 (Abcam, Cambridge, MA), Biotinylated Goat anti-Rabbit secondary antibody (Vector) and Avidin-conjugated peroxidase (Vectastain ABC kit, Vector); staining was visualized with ImmPACT DAB Peroxidase Substrate (Vector). Sections were counterstained with hematoxylin and mounted with Permount (Fisher, Pittsburgh, PA). Alternatively, β-catenin staining was detected by Goat anti-Rabbit/Alexa Fluor 594 antibody, and the sections counterstained with Hoechst 33342 and mounted with Fluoromount-G.

miRNA expression profiling in the liver. Livers from WT C57BL/6 mice were isolated at E15.5 (n = 3; mixed gender), 2w (n = 3; male), 3w (n = 3, male) and 7w (n = 3; male). Differential miRNA expression was assessed using the nCounter Mouse miRNA Expression Assay Kit (NanoString, Seattle, WA). Hybridization was performed by the Genomics Research Core at the University of Pittsburgh, according to manufacturer's instructions with 100 ng of total RNA per reaction. Hybridized probes were purified using the nCounter prep station, and cartridges were scanned on the nCounter Digital Analyzer. High-density scan settings were used (600 fields-of-view per sample). Raw data were normalized using nSolver Analysis Software 2 (NanoString) based on the counts of four miRNAs that were observed to be relatively consistent at all ages: miR-16, miR-34c, miR-155 and miR-741. Using Partek Genomics Suite 6.6 (Partek, St. Louis, MO), background values (i.e., the mean of negative control values + 3 standard deviations) were subtracted from each sample, allowing the identification of 99.86% of background noise. miRNAs with background values for all samples analyzed were deleted; in contrast, all other miRNA counts with negative values were "floored" to a minimum value of 0.001. Data were $\log_2$ transformed. Data were filtered for miRNAs differentially expressed at ages E15.5, 2w and 3w compared to 7w with fold change <1.5 or >1.5 and P value with false discovery rate < 0.05, as determined by ANOVA. Primary data files (#GSE68537) are available at Gene Expression Omnibus.

Identification of cytokinesis-associated genes targeted by the subset of miRNAs elevated during liver postnatal development. Ingenuity Pathway Analysis (IPA) (version 24718999; Qiagen, Redwood City, CA) classifies 323 genes as "affecting" or "activating" cytokinesis. The 3'UTRs of these cytokinesis-associated genes were screened using TargetScan 6.2 for seed matching sequences to each of the miRNAs up-regulated during postnatal development (see Supporting Table 1). Among these 60 miRNAs, miR-1937a and -1937c were excluded from analysis because they are actually tRNA fragments (personal communication, Peterson K, miRBase.org); miR-2134, an rRNA fragment, was also excluded (1). Target genes were identified by the presence miRNA-specific seed sequences within the 3'UTR of each mouse gene. Supporting Table 2 summarizes all miRNAs elevated during postnatal development and their predicted cytokinesis-associated target genes.

Identification of candidate cytokinesis genes with miR-122 seed matching sequences. We utilized published data to identify miR-122 target genes that regulate cytokinesis. We started with genes that were

differentially expressed in 10w-old *Mir122*-LKO livers compared to controls (*n* = 5; Gene Expression Omnibus identifier GSE20610) (2). IPA revealed 63 cytokinesis-associated genes (categories "activating" and "affecting" cytokinesis) that were differentially expressed in *Mir122*-LKO livers and statistically significant ($P < 0.05$) (Supporting Table 3). Using TargetScan 6.2 (3) and/or MiRanda (August 2010 release) prediction algorithms (4), we identified genes with conserved miR-122 seed matching sequences that were also up-regulated ≥1.3-fold (*Mapre1, Nedd4l, Rhoa* and *Vps4a*) (Supporting Table 4). Next, we interrogated the 427 genes identified by Neumann et al. (5) that promote cytokinesis failure or binucleation and identified 31 genes up-regulated in *Mir122*-LKO livers ($P < 0.05$) (Supporting Table 5). Using TargetScan and/or MiRanda, we identified genes with conserved miR-122 seed matching sequences that were also up-regulated ≥1.3-fold (*Galc, Nedd4l* and *Slc25a34*). Finally, by searching the literature, we identified additional candidate genes (*Cux1, Iqgap1, Mapre1 and Rhoa)* based on two criteria: (a) up-regulation in *Mir122*-deficient livers and (b) association with cytokinesis.

miR-122 adenovirus production. miR-122 adenovirus was generated by first PCR amplifying pre-miR-122 from C57BL/6 mouse genomic DNA using Phusion HF DNA polymerase (New England Biolabs, Ipswich, MA). The total 256 base pair (bp) product contained the miR-122 stem loop (67 bp) and 100 bp sequence upstream and downstream of the stem loop. The following primers were used. Lowercase sequences correspond to restriction digestion sites, and uppercase sequences correspond to genomic DNA.

- (forward) BamHI.XbaI.pre-miR122: cgggatcccgtctaga-GCAGTTTCAGCGTTTGGAACCA
- (reverse) NheI.pre-miR122: tcgagctagc-TACATTACACACAATGGAGAA

The PCR product and pacAd5-GFP/Puro vector (Cell Biolabs, San Diego, CA) were digested with BamHI + NheI (New England Biolabs) and ligated with T4 ligase (Life Technologies). Three additional copies of pre-miR-122 were cloned in tandem, resulting in an adenoviral expression construct with four consecutive pre-miR-122 sequences: pacAd5-miR122x4-GFP/Puro. miR-122 adenovirus (Ad-miR122) and control adenovirus (Ad-control) were generated by transfecting pacAd5-miR122x4-GFP/Puro or pacAd5-GFP/Puro, respectively, into 293A cells (ATCC, Manassas, VA) and generating virus using manufacturer's recommendations (RAPAd miRNA Adenoviral Expression System, Cell Biolabs). See Supporting Fig. 7A. Viral particles were purified using Fast Trap Adenovirus Purification and Concentration Kit (Millipore, Billerica, MA), and the number of viral particles calculated based on optical density readings at 260 nm (OD_{260}) (AdenoVator Vector System, Qbiogene, Carlsbad, CA). Adenovirus activity was validated *in vitro.* Freshly isolated hepatocytes from 2.5mo-old *Mir122*-KO (n = 3) were cultured using our standard hepatocyte culture conditions. Cells were infected with Ad-miR122 or Ad-control (0.6 x 109 viral particles) on day 1 and miR-122 levels determined by qRT-PCR on day 6.

Adenovirus-mediated expression of miR-122 in Mir122-KO livers. Twelve-day old *Mir122*-KO mice weighing 7-8g were transduced with Ad-miR122 or Ad-control (intraperitoneal injection with 1×10^9 viral particles; *n* = 5 mice/injection) (see Fig. 4E). Livers were harvested on postnatal day 22, fixed with 4% PFA and embedded in paraffin. Liver sections were stained with anti-β-catenin antibody + Hoechst 33342 to quantify binucleate hepatocytes or anti-Ki-67 antibody to identify proliferating cells.

Hepatocyte isolation. Hepatocytes from 14-15d-old or adult mice were isolated using two-step collagenase perfusion (6). Briefly, a catheter was inserted into the portal vein or interior vena cava and 0.3 mg/ml collagenase II (Worthington, Lakewood, NJ) circulated through the liver. Digested livers were placed in DMEM-F12 with 15 mM HEPES (Corning, Corning, NY) + 5% FBS (Atlanta Biologicals, Norcross, GA), passed through a 70 μm cell strainer and centrifuged 2-3 times at 55g for 3 min. to remove non-parenchymal cells. Hepatocyte viability, determined by trypan blue staining, was typically >85%.

Ploidy analysis. First, freshly isolated primary hepatocytes were washed twice in PBS, adjusted to a density of 5-10 million cells/ml and incubated on ice for 30 min. with 2 μl/ml Fixable Viability Dye (FVD) eFluor 780 (eBioscience, San Diego, CA). Secondly, after 3 washes with PBS, hepatocytes were fixed with 2% PFA for 20 min. at room temperature. Next, hepatocytes were washed 3 times in PBS and incubated with permeabilization buffer (0.1% saponin and 0.5% BSA in PBS) for 10 min. at room temperature. Finally, hepatocytes were

incubated with 15 µg/ml Hoechst 33342 at room temperature for 30 min. Cells were washed twice and stored in permeabilization buffer. Ploidy analysis was performed with a FACS Aria II-SORP (BD Biosciences, San Jose, CA) equipped with a 130 um nozzle and running DiVa v8 software. Cells that were dead prior to fixation were excluded on the basis of positive FVD staining. Doublets were excluded. FACS plots were generated using FlowJo 9.8 (Treestar, Ashland, OR).

Hepatocyte karyotypes. Primary hepatocytes were cultured for 40h and arrested in metaphase, as described previously (7). Chromosomes were G-banded using standard trypsin/Wright's methodology and karyotypes determined for 20 hepatocytes/sample. All karyotypes were prepared and interpreted by the Cytogenetics Research Service Laboratory at Oregon Health and Science University (Portland, OR).

In vitro proliferation of diploid hepatocytes. Hepatocytes from 14-15d-old WT C57BL/6 mice were seeded at 40,000 viable cells/well in 24-well Primaria Cell Culture plates (Corning) in growth media: DMEM-F12 with 15 mM HEPES (Corning), 5% FBS (Atlanta Biologicals), Antibiotic-Antimycotic Solution (Corning) and ITS Supplement (containing 5 µg/ml insulin, 5 µg/ml transferrin and 5 ng/ml sodium selenite; Roche). After 16h, growth media was replaced with fresh media lacking Antibiotic-Antimycotic Solution, and cells were transfected with 25 nm or 200 nM miRIDIAN miR-122 mimic (Fisher, C-300591-05-0005) or miRIDIAN negative control (Fisher, CN-001000-01-05) using Lipofectamine 2000 (Life Technologies). Alternatively, cells were transfected with 20-40 nM stealth siRNAs from Life Technologies using Lipofectamine RNAiMAX: negative "scramble" control (12935-300), *Racgap1* (MSS219011)*, Cux1* (MSS203376)*, Rhoa* (HSS100656; the product ID refers to a human siRNA, but it also targets mouse), *Mapre1* (MSS274053)*, Iqgap1* (MSS219911)*, Nedd4l* (MSS234761) and *Slc25a34* (MSS242504). Six hours after transfection, media was replaced with fresh growth media containing 0.5% FBS. Cultures were assessed for proliferation and cell death on days 2, 3 and 4 (see the timeline in Figs. 4A,6A) according to manufacturers' instructions. Morphological changes were documented in cultures fixed with 4% PFA and stained with Hoechst 33342 using phase contrast microscopy (to visualize cell borders) and fluorescent microscopy (to visualize nuclei). For BrdU labeling (a measure of S-phase), hepatocytes were cultured in growth media containing 1 mM BrdU (Sigma-Aldrich, St. Louis, MO) for 24h prior to harvest, fixed in 4% PFA and incubated with anti-BrdU antibody (BD Biosciences), Goat anti-Mouse/Alexa Fluor 594 secondary antibody (Life Technologies) and Hoechst 33342. A minimum of 250 cells/sample was scored. For phospho-histone H3 (PHH3) staining, cultures were fixed in 4% PFA and stained with anti-PHH3 antibody (Cell Signaling Technology, Danvers, MA), Goat anti-Rabbit/Alexa Fluor 594 secondary antibody (Life Technologies) and Hoechst 33342. Nuclei with punctate PHH3 staining were considered to be in G_2-phase. A minimum of 500 cells/sample was scored. For measuring apoptosis, hepatocytes were cultured in growth media containing 5 µM NucView 488 substrate (a substrate for detecting active caspase-3, a marker of apoptosis; Biotium, Hayward, CA) for 20 min. before harvest. Cells were then fixed with 4% PFA and stained with Hoechst 33342. At least 500 cells/sample were scored. The number of mono-, bi- and multinucleate hepatocytes was quantified on day 4. Because of difficulty discerning individual hepatocytes in tightly packed clusters, single cell suspensions were obtained by trypsinization, fixed with 4% PFA and cytospun onto slides. Cells were then stained with Hoechst 33342. Individual cells were easily observed (see Supporting Figs. 6,11). At least 500 cells/samples was scored in a blinded fashion.

Luciferase assay. Mapre1, Iqgap1, Nedd4l and Slc25a34 3'UTR regions were amplified from mouse genomic DNA using Phusion HF DNA polymerase (New England Biolabs). Full length 3'UTR (containing miR-122 seed match sequences) and truncated 3'UTR (with miR-122 seed match sequences deleted) regions were amplified for each gene, as described in Supporting Fig. 8. Primer sequences are listed below. PCR products were directionally cloned into psiCHECK2 vector (Promega, Madison, WI) using XhoI and NotI (New England Biolabs) restriction sites at the 5' and 3' ends, respectively. For the luciferase assay, NIH3T3 cells (ATCC, Manassas, VA) were transfected simultaneously with 200 ng luciferase reporter construct and 25 nM miRIDIAN miR-122 mimic (Fisher, C-300591-05-0005) or miRIDIAN negative control (Fisher, CN-001000-01-05) using Lipofectamine 2000 (Life Technologies). Transfected cells were harvested after 48h and processed with Dual-Luciferase Reporter Assay kit (Promega). Luciferase activity was detected with an Infinite M200 PRO

microplate reader (Tecan, Männedorf, Switzerland). Relative luciferase activities of transfected plasmids are represented as the activity of *Renilla* luciferase activity normalized to firefly activity.

RNA isolation and quantitative reverse transcriptase PCR (qRT-PCR). Total RNA was isolated from liver tissues using Trizol (Life Technologies) and subjected to the qRT-PCR to quantify the expression of miRNAs and protein-coding genes. Mature miRNAs were amplified and quantified using Taqman miRNA probes (Life Technologies) and Taqman Universal Master Mix II (Life Technologies). For protein-coding genes, total RNA was first reverse-transcribed into complementary DNA using M-MLV (Life Technologies) and quantitative PCR reaction performed with SYBR Green PCR Master Mix (Life Technologies). Taqman probe IDs and primer sequences are listed below. Reactions were performed using a StepOnePlus System (Life Technologies). Relative expression was calculated using ΔΔCT method (8).

Western Blotting. Whole cell lysates were extracted from manual homogenization of frozen liver tissue using sodium dodecyl sulfate (SDS)-based lysis buffer (50 mM Tris-HCl, pH 8.0, 10 mM EDTA, 1%SDS) containing protease/phosphatase inhibitors. Lysates were removed to a fresh 1.5 ml tube and centrifuged at 18.4g for 10 min. at 4^{o}C in order to remove clear supernatant to a new 1.5 ml tube while disposing of the pellet. Samples were stored at -80^{o}C until utilization or determination of protein concentration via BCA protein assay (Fisher) to ensure equal protein concentrations for subsequent assays. Lysate (100 µg) was run on precast 4-14% gradient polyacrylamide gels (Bio-Rad, Hercules, CA) at 60V for 15 min., then 120V for 1.5h. Gels were then transferred onto a polyvinylidene fluoride (PVDF) membrane (Millipore) for 1h at 4^{o}C using 100V. Membranes were blocked in 5% non-fat dry milk dissolved in Blotto (0.15M NaCl, 0.02M Tris pH 7.5, 0.1% Tween in dH_2O) for 1h at room temperature. Primary antibodies were diluted in 5% milk/Blotto or 5% BSA/Blotto according to manufacturers' recommendations and incubated on membranes overnight at 4^{o}C while shaking. Primary antibodies used for western blotting were the following: anti-Racgap1 (Fisher), anti-Cux1 (Santa Cruz), anti-Rhoa (Cell Signaling Technology), anti-Mapre1 (Santa Cruz), anti-Iqgap1 (Santa Cruz), anti-Nedd4l (Cell Signaling Technology), anti-Slc25a34 (Sigma Aldrich), anti-β-actin (Abcam) and anti-Gapdh (Santa Cruz). Membranes were then washed in Blotto for 1h at room temperature prior to incubation of membranes with Donkey anti-Rabbit Horseradish peroxidase secondary antibody (GE Healthcare Life Sciences, Pittsburgh, PA) diluted 1:5,000 in respective 1% milk or 1% BSA for one hour. Membranes were again washed in Blotto for 1h at room temperature prior to expose to SuperSignal West Pico Chemiluminescent Substrate (Thermo Scientific Pierce, Pittsburgh, PA) for 1-2 min. at room temperature. The bands reflective of target proteins were viewed by ChemiDoc imaging system (Bio-Rad) and quantified with ImageJ (National Institutes of Health, Bethesda, MD). The antibodies used were listed in supporting information.

Detailed information for select reagents:

Primer pairs for qRT-PCR

Gene	*Forward primer (5' to 3')*	*Reverse primer (5' to 3')*
Cux1	TCTCTATCAGCCTCTCACTCCGTC	CCTGTTTGCCAATACTGTTGCG
Ect2	AACTTGTGCTTGGCGTCTAC	TTTTTCCTCCGATTTTCCAGG
Gapdh	TCCTGCACCACCAACTGCTTAG	TGCTTCACCACCTTCTTGATGTC
Iqgap1	TTCTCTCCCAAAGTGGTGTCCC	TCTTAGGCAACCCAATCTCATCC
Kif23/Mklp1	ATGTGAGCGTAGAGTGGCAG	GCCGTTGGAAATCTGAGCAA
Mapre1	TGATTTGCCAGGAGAACG	GCCCCCTTCATCAGGTATCA
Nedd4l-long	CGACGCACTTCAGCCAGT	CTTCTTGGCGAGGTCAATTC
Nedd4l-short	AGAGGGCTCTGCCTGGTGGG	CGAGTGGGCGGAGCAAGGTG
Racgap1	CGGGAAGTCAGGACCTTTACAAC	TGGATGGGAGACCAAACGACAGTC
Rhoa	CAGGTAGAGTTGGCTTTGTGGG	TCCCGCCTTGTGTGCT
Slc25a34	ACAATCAGCCAGTGGACAGAGC	TCGCAACCAGTTTCCGAAGC

Taqman probes for qRT-PCR

miRNA or *control*	*Vendor*	*Assay ID*
mmu-miR-16-5p	Life Technologies	000391
mmu-miR-23a-3p	Life Technologies	000399
mmu-miR-30d-5p	Life Technologies	000420
mmu-miR-122-5p	Life Technologies	002245
mmu-miR-148a-3p	Life Technologies	000470
mmu-miR-194-5p	Life Technologies	000493
RNU6b	Life Technologies	001093

Luciferase constructs

Construct	*Forward primer (5' to 3')**	*Reverse primer (5' to 3')***
Iqgap1		
FL	CCGCTCGAGTGCAGCTACAGTATGAAGGAGTTGC	ATAAGAATGCGGCCGCGGCTTATGGCTTCACAAGGAGA
DEL	CCGCTCGAGTGCAGCTACAGTATGAAGGAGTTGC	ATAAGAATGCGGCCGCCGAGCGACCCATTACTTCCCAT
Mapre1		
FL	CCGCTCGAGAGCAGAGCAACATCCGAAG	AAGAATGCGGCCGCTGACAATGGGGAGCAGTGAC
DEL	CCGCTCGAGCAGAAGTCTCACCTTTTCCG	AAGAATGCGGCCGCTGACAATGGGGAGCAGTGAC
Nedd4l		
FL	CCGCTCGAGCGTTGCCTAAAATGCCCGATG	ATAAGAATGCGGCCGCGGACTTCACTTTGTCACAGTTCCC
DEL	CCGCTCGAGCGTTGCCTAAAATGCCCGATG	ATAAGAATGCGGCCGCTAGCCTTCCTTCTGTTGAGGGG
Slc25a34		
FL	CCGCTCGAGTTCGGAAACTGGTTGCGAGG	ATAAGAATGCGGCCGCGCTTGAGATTGAGGGTTTGGG
DEL	CCGCTCGAGTTCGGAAACTGGTTGCGAGG	ATAAGAATGCGGCCGCCGTACACAAACAGGAAGCCTGGAC

* Underlined sequences contain a NotI restriction site plus 3 additional bases at the 5' end.

** Underlined sequences contain an XhoI restriction site plus 8 additional bases at the 5' end.

Antibodies and associated reagents

Antibodies and associated reagents	*Vendor*	*Catalog #*
β-actin antibody	Abcam	ab8227
β-catenin antibody	Santa Cruz	sc-7199
Biotinylated goat anti-rabbit antibody	Vector Laboratories	BA-1000
BrdU antibody	BD Biosciences	347580
Cux1 antibody	Santa Cruz	sc-13024
Donkey anti-Goat/Alexa Fluor 594 antibody	Life Technologies	A-11058
Donkey anti-Rabbit/Horseradish peroxidase	GE Healthcare Life Sciences	NA934
Gapdh antibody	Santa Cruz	sc-25778
Goat anti-Mouse/Alexa Fluor 488 antibody	Life Technologies	A-11029
Goat anti-Mouse/Alexa Fluor 594 antibody	Life Technologies	A-11005
Goat anti-Rabbit/Alexa Fluor 488 antibody	Life Technologies	A-11034
Goat anti-Rabbit/Alexa Fluor 594 antibody	Life Technologies	A-11012
Iqgap1 antibody	Santa Cruz	sc-10792
Ki-67 antibody	Abcam	ab15580
Mapre1 antibody	Santa Cruz	sc-15347
Nedd4l antibody	Cell Signaling Technology	4013
PCNA antibody	Santa Cruz	sc-56
Phalloidin/Alexa Fluor 488	Life Technologies	A-12379
Phospho-histone H3 antibody	Cell Signaling Technology	9701
Racgap1 antibody	Thermo Scientific	PA5-22265
Rhoa antibody	Cell Signaling Technology	2117
Slc25a34 antibody	Sigma Aldrich	SAB2102187
Streptavidin/Alexa Fluor 488	Life Technologies	S-11223

Supporting References

1. Chiang HR, Schoenfeld LW, Ruby JG, Auyeung VC, Spies N, Baek D, Johnston WK, et al. Mammalian microRNAs: experimental evaluation of novel and previously annotated genes. Genes Dev 2010;24:992 1009.
2. **Hsu SH**, **Wang B**, **Kota J**, **Yu J**, **Costinean S**, **Kutay H**, **Yu L**, et al. Essential metabolic, anti-inflammatory, and anti-tumorigenic functions of miR-122 in liver. J Clin Invest 2012;122:2871-2883.
3. Lewis BP, Burge CB, Bartel DP. Conserved seed pairing, often flanked by adenosines, indicates that thousands of human genes are microRNA targets. Cell 2005;120:15-20.
4. Enright AJ, John B, Gaul U, Tuschl T, Sander C, Marks DS. MicroRNA targets in Drosophila. Genome Biol 2003;5:R1.
5. **Neumann B**, **Walter T**, Heriche JK, Bulkescher J, Erfle H, Conrad C, Rogers P, et al. Phenotypic profiling of the human genome by time-lapse microscopy reveals cell division genes. Nature 2010;464:721-727.
6. Overturf K, Al-Dhalimy M, Tanguay R, Brantly M, Ou CN, Finegold M, Grompe M. Hepatocytes corrected by gene therapy are selected in vivo in a murine model of hereditary tyrosinaemia type I. Nat Genet 1996;12:266-273.
7. Duncan AW, Hanlon Newell AE, Bi W, Finegold MJ, Olson SB, Beaudet AL, Grompe M. Aneuploidy as a mechanism for stress-induced liver adaptation. J Clin Invest 2012;122:3307-3315.
8. Livak KJ, Schmittgen TD. Analysis of relative gene expression data using real-time quantitative PCR and the 2(-Delta Delta C(T)) Method. Methods 2001;25:402-408.

Author names in bold designate shared co-first authorship.

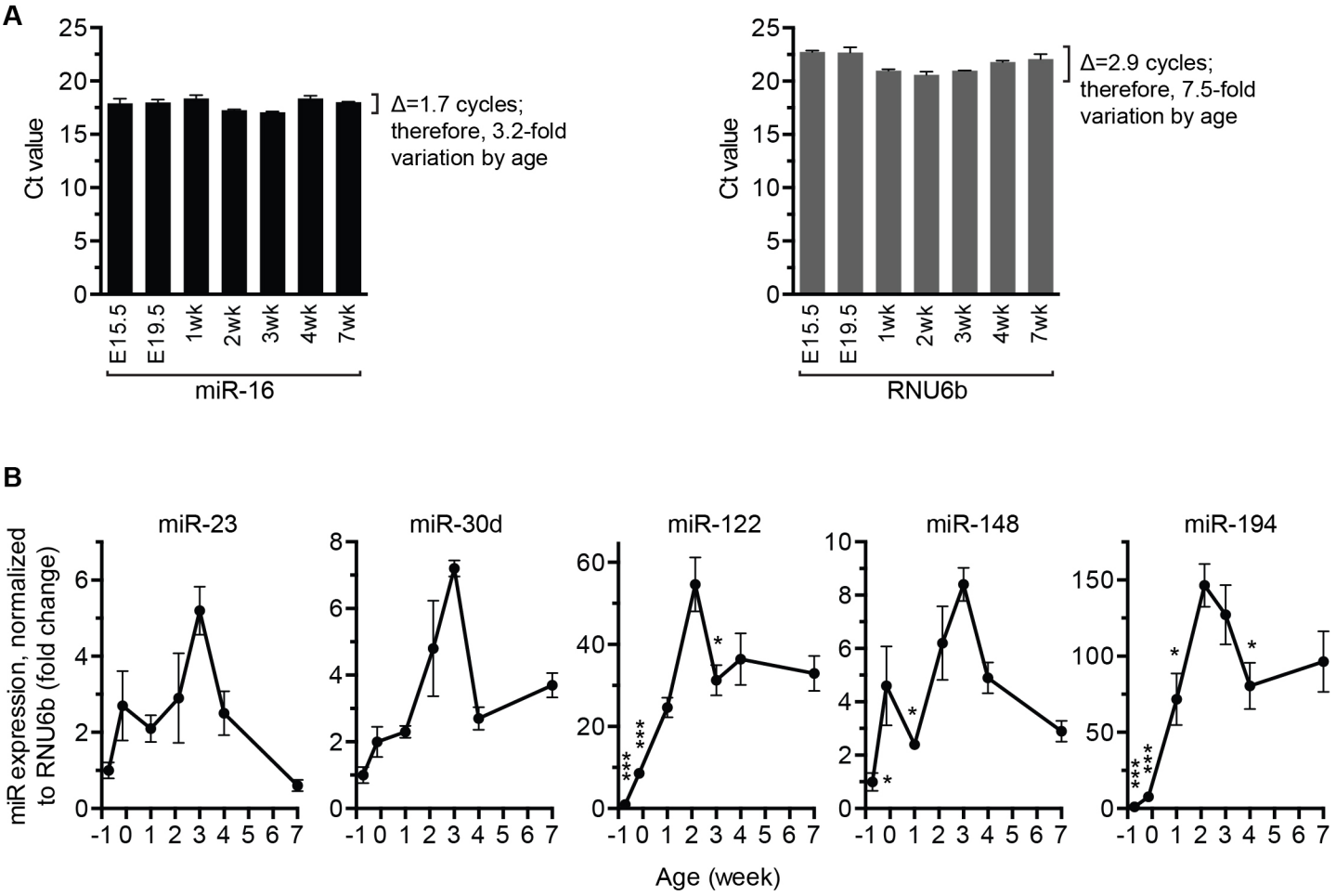

Supporting Fig. 1. miR-16 expression is nearly constant in embryonic, postnatal and adult livers. (A) miR-16 and RNU6b expression was examined by qRT-PCR in WT C57BL/6 mouse livers ages E15.5 to 7wk (n = 3-4). Cycle threshold (Ct) values for miR-16 were relatively constant, changing only 1.7 cycles over the age range. In contrast, RNU6b Ct values displayed greater variation (2.9 cycles). (B) Expression of select miRNAs (elevated during postnatal development) was tracked in WT C57BL/6 livers at ages E15.5, E19.5, 1-, 2-, 3-, 4- and 7wk (n = 3-5) by qRT-PCR. Peak expression of miR-23, -30d, -122, -148 and -194 occurred at 2-3wks. Expression values were normalized to RNU6b. * $P \leq 0.04$, ** $P \leq 0.009$, *** $P < 0.0008$, compared to 2wk. Graphs show mean ± SEM.

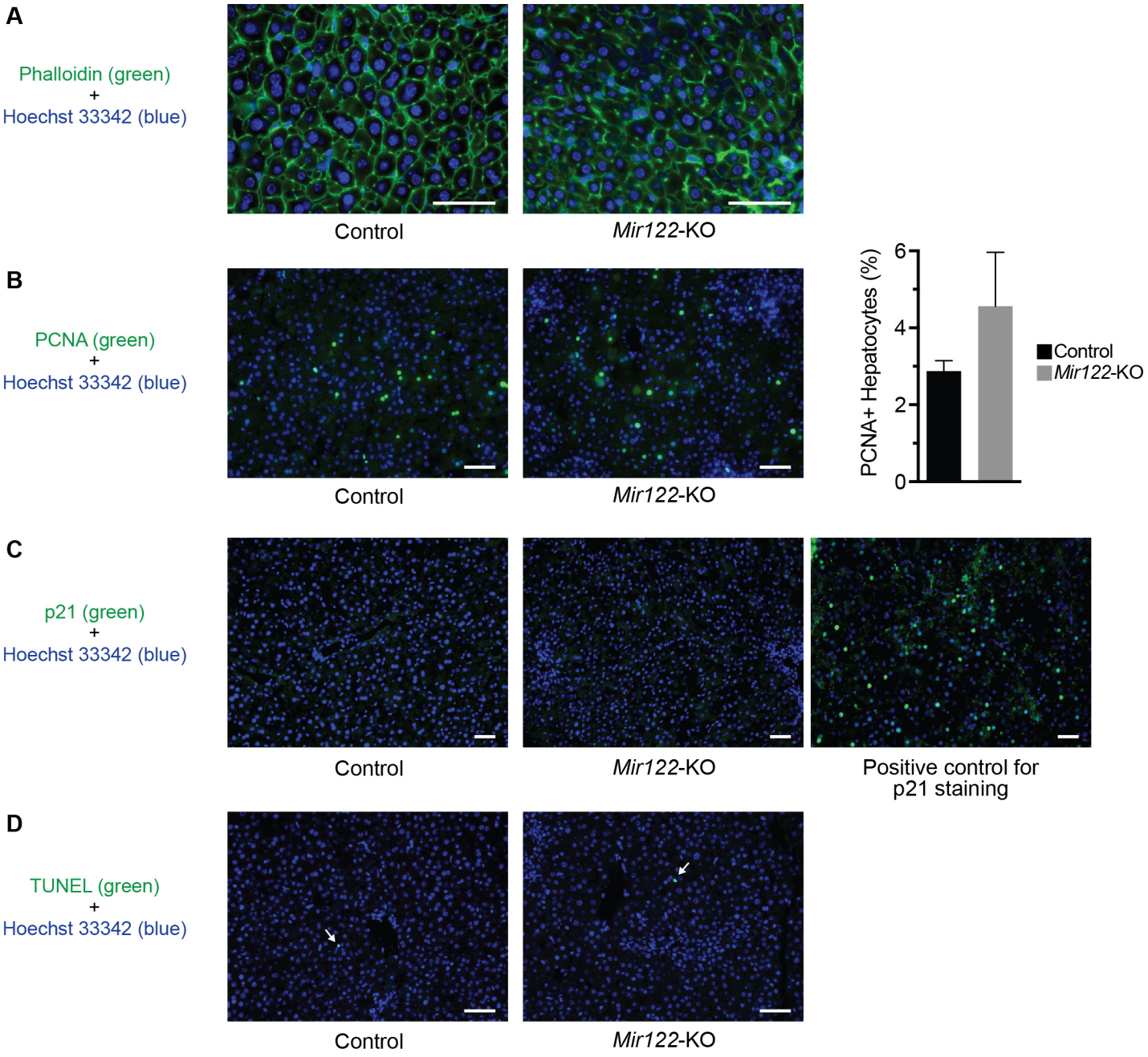

Supporting Fig. 2. Loss of miR-122 does not affect proliferation, p21-mediated cell cycle arrest or death in the liver. (A) Livers from 28d-old control or *Mir122*-KO mice (n = 4-5) were stained with phalloidin to mark cell boundaries and Hoechst 33342 to mark nuclei and the number of mono- and binucleate hepatocytes counted. Representative images are shown and the percentage of binucleate hepatocytes reported in Fig. 3A. (B-D) Liver sections from 28d-old control or *Mir122*-KO mice (n = 4-5) were stained for the proliferation marker PCNA, the cell cycle arrest marker p21 and the apoptosis assay TUNEL. PCNA (B), p21 (C) and TUNEL (D) staining was equivalent in control and *Mir122*-KO livers. WT mice treated with streptozotocin were used as a positive control for p21 staining (Mol Nutr Food Res 2009;53:859). Arrows indicate TUNEL positive cells. Representative images are shown. Scale bars are 50 μm. The graph shows mean ± SEM.

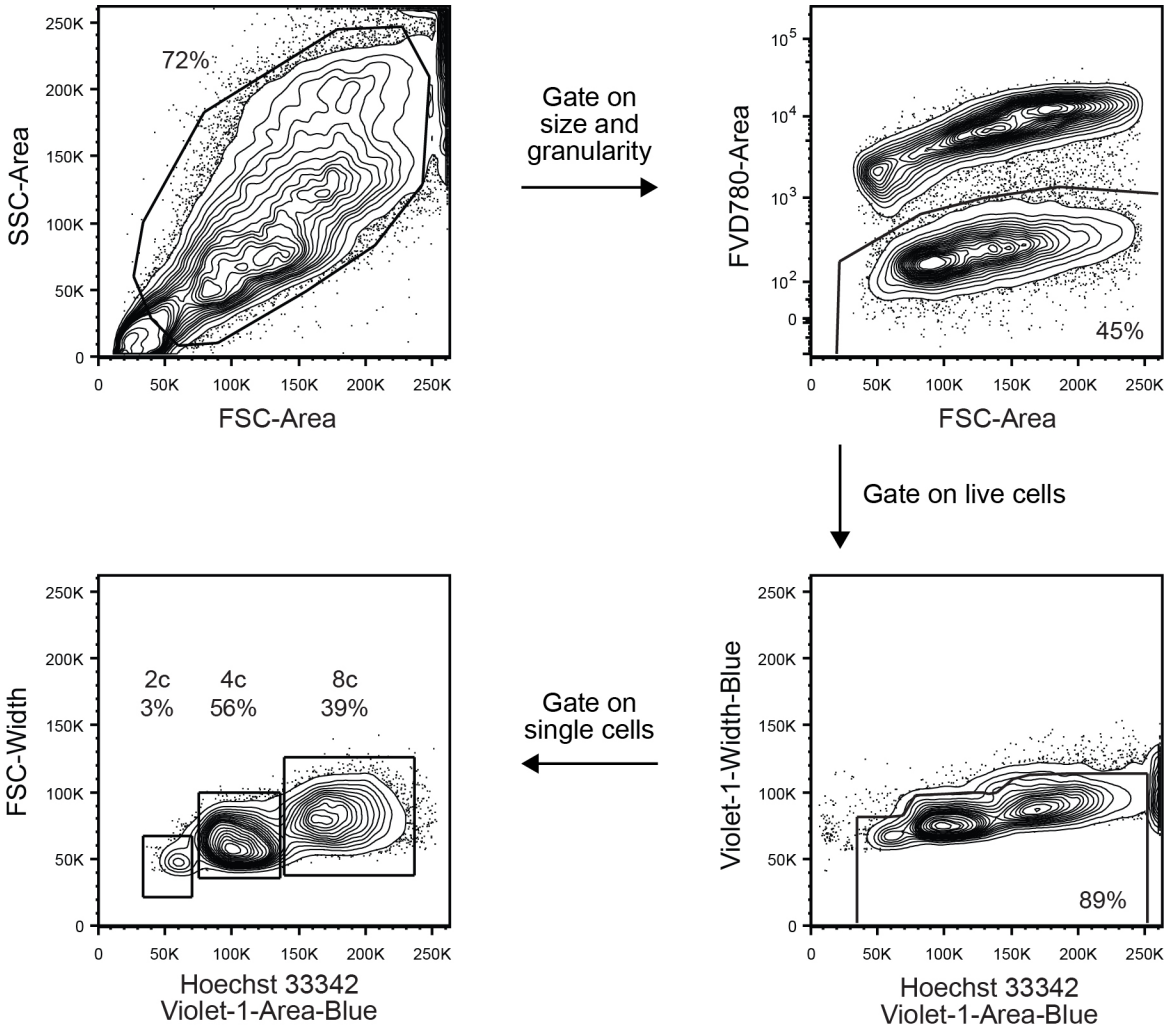

Supporting Fig. 3. Gating strategy for identification of hepatocyte ploidy populations by flow cytometry. Representative gating is shown for *Mir122*-control hepatocytes.

A

Control hepatocytes, mouse 1

Aneu-ploid	Nearest Ploidy	Chr Number	Sex Chr	Chr Losses	Chr Gains	Additional Abnormalities
	2n	40	XY			
yes	4n	74	XXYY	2, 3x2, 4, 11, 15		
yes	4n	77	XXYY	1, 6, 7		
yes	4n	78	XXYY	8, 17		
yes	4n	78	XXYY	8, 13, 17	18	
yes	4n	78	XXYY	9, 11		
yes	4n	78	XXYY	5, 16		
yes	4n	79	XXYY	19		
yes	4n	79	XXYY	17		
yes	4n	79	XXYY	7		Del(8), Del(18)
yes	4n	79	XXYY	7		
yes	4n	79	XXYY	5		
	4n	80	XXYY			
	4n	80	XXYY			
	4n	80	XXYY			
	4n	80	XXYY			
yes	4n	80	XXYY	10	5	
	4n	80	XXYY			
yes	4n	81	XXYY		17	
yes	4n	82	XXYY		2, 10	

Control hepatocytes, mouse 2

Aneu-ploid	Nearest Ploidy	Chr Number	Sex Chr	Chr Losses	Chr Gains	Additional Abnormalities
yes	4n	76	XXY	2, 8, 13, Y		
yes	4n	76	XXYY	5, 10, 13, 19		
yes	4n	76	XXYY	4, 5, 6x2,	Mar	
yes	4n	76	XXYY	7, 9, 10, 15		
yes	4n	77	XXYY	2, 13, 16		
yes	4n	78	XXYY	1x2		
yes	4n	78	XXYY	4, 14		
yes	4n	78	XXYY	2, 15		
yes	4n	79	XXYY	8		
yes	4n	79	XXYY	19		
yes	4n	79	XXY	Y		
yes	4n	79	XXYY	13		
	4n	80	XXYY			
	4n	80	XXYY			
	4n	80	XXYY			
	4n	80	XXYY			
	4n	80	XXYY			
	4n	80	XXYY			
	4n	80	XXYY			
	4n	80	XXYY			
	4n	80	XXYY			

Control hepatocytes, mouse 3

Aneu-ploid	Nearest Ploidy	Chr Number	Sex Chr	Chr Losses	Chr Gains	Additional Abnormalities
yes	2n	37	XY	7, 15x2		
yes	2n	38	XY	7, 12		
yes	2n	39	XY	17		
	2n	40	XY			
	2n	40	XY			
yes	4n	72	XXYY	1, 4, 7, 8, 9, 10, 11, 15		
yes	4n	73	XXYY	3x2, 5, 12, 13, 14, 17		
yes	4n	75	XXYY	3, 6, 10, 15, 16		
yes	4n	76	XY	4, 7, X, Y		
yes	4n	78	XXYY	11, 14		
yes	4n	79	XXYY	11		
yes	4n	79	XXYY	2, 19	15	
yes	4n	79	XXYY	18		
yes	4n	79	XXY	Y		
	4n	80	XXYY			
	4n	80	XXYY			
	4n	80	XXYY			
	4n	80	XXYY			
	4n	80	XXYY			
	4n	80	XXYY			

Control hepatocytes, mouse 4

Aneu-ploid	Nearest Ploidy	Chr Number	Sex Chr	Chr Losses	Chr Gains	Additional Abnormalities
yes	2n	39	X	Y		
	2n	40	XY			
yes	3n	69	XXY	12	4, 5, 7, 8, 9, 10, 13, 15, 16, 17, 18	Rb(5.16)
yes	4n	74	XXY	7x2, 9, 12,		
yes	4n	77	XXYY	4, 5, 19		
yes	4n	78	XXYY	9, 11		
yes	4n	78	XXYY	18, 19		
yes	4n	79	XXY	Y		
yes	4n	79	XXYY	19		
	4n	79	XXY			
	4n	80	XXYY			
	4n	80	XXYY			
	4n	80	XXYY			
	4n	80	XXYY			
	4n	80	XXYY			
	4n	80	XXYY			
	4n	80	XXYY			
yes	4n	80	XXYY	13	18	
	4n	80	XXYY			
yes	4n	81	XXYY		18	Der(18)

Supporting Fig. 4. Karyotypes of control and *Mir122*-KO hepatocytes. Hepatocytes isolated from 2.5mo-old control and *Mir122*-KO livers were karyotyped by G-banding. Karyotypes are shown for control (A) and *Mir122*-KO (B) hepatocytes (*n* = 4 mice/genotype; *n* = 20 karyotypes/mouse). The overall degree of aneuploidy is reported in Fig. 3F.

B

Mir122-KO hepatocytes, mouse 1

Aneu-ploid	Nearest Ploidy	Chr Number	Sex Chr	Chr Losses	Chr Gains	Additional Abnormalities
yes	2n	39	X	Y		
yes	2n	39	XY	6		
	2n	40	XY			
	2n	40	XY			
	2n	40	XY			
	2n	40	XY			
	2n	40	XY			
	2n	40	XY			
	2n	40	XY			
	2n	40	XY			
	2n	40	XY			
	2n	40	XY			
	2n	40	XY			
	2n	40	XY			
	2n	40	XY			
	2n	40	XY			
	2n	40	XY			
	2n	40	XY			
	2n	40	XY			
	4n	80	XXYY			
	4n	80	XXYY			

Mir122-KO hepatocytes, mouse 2

Aneu-ploid	Nearest Ploidy	Chr Number	Sex Chr	Chr Losses	Chr Gains	Additional Abnormalities
yes	2n	38	XY	7, 13		
yes	2n	39	XY	19		
yes	2n	39	XY	17		
	2n	40	XY			
	2n	40	XY			
	2n	40	XY			
	2n	40	XY			
	2n	40	XY			
	2n	40	XY			
	2n	40	XY			
	2n	40	XY			
	2n	40	XY			
	2n	40	XY			
	2n	40	XY			
	2n	40	XY			
	2n	40	XY			
	2n	40	XY			
	2n	40	XY			
	2n	40	XY			
	4n	80	XXYY			

Mir122-KO hepatocytes, mouse 3

Aneu-ploid	Nearest Ploidy	Chr Number	Sex Chr	Chr Losses	Chr Gains	Additional Abnormalities
yes	2n	39	XY	19		
	2n	40	XY			
	2n	40	XY			
	2n	40	XY			
	2n	40	XY			
	2n	40	XY			
	2n	40	XY			
	2n	40	XY			
	2n	40	XY			
	2n	40	XY			
	2n	40	XY			
	2n	40	XY			
	2n	40	XY			
	2n	40	XY			
	2n	40	XY			
	2n	40	XY			
	2n	40	XY			
	2n	40	XY			
yes	4n	79	XXYY	1		
	4n	80	XXYY			

Mir122-KO hepatocytes, mouse 4

Aneu-ploid	Nearest Ploidy	Chr Number	Sex Chr	Chr Losses	Chr Gains	Additional Abnormalities
yes	2n	38	X	16, Y		
yes	2n	39	XY	15		
yes	2n	39	XY	13		
	2n	40	XY			
	2n	40	XY			
	2n	40	XY			
	2n	40	XY			
	2n	40	XY			
	2n	40	XY			
	2n	40	XY			
	2n	40	XY			
	2n	40	XY			
	2n	40	XY			
	2n	40	XY			
	2n	40	XY			
	2n	40	XY			
	2n	40	XY			
	2n	40	XY			
	2n	40	XY			
	2n	40	XY			

Supporting Fig. 4 *(continued).*

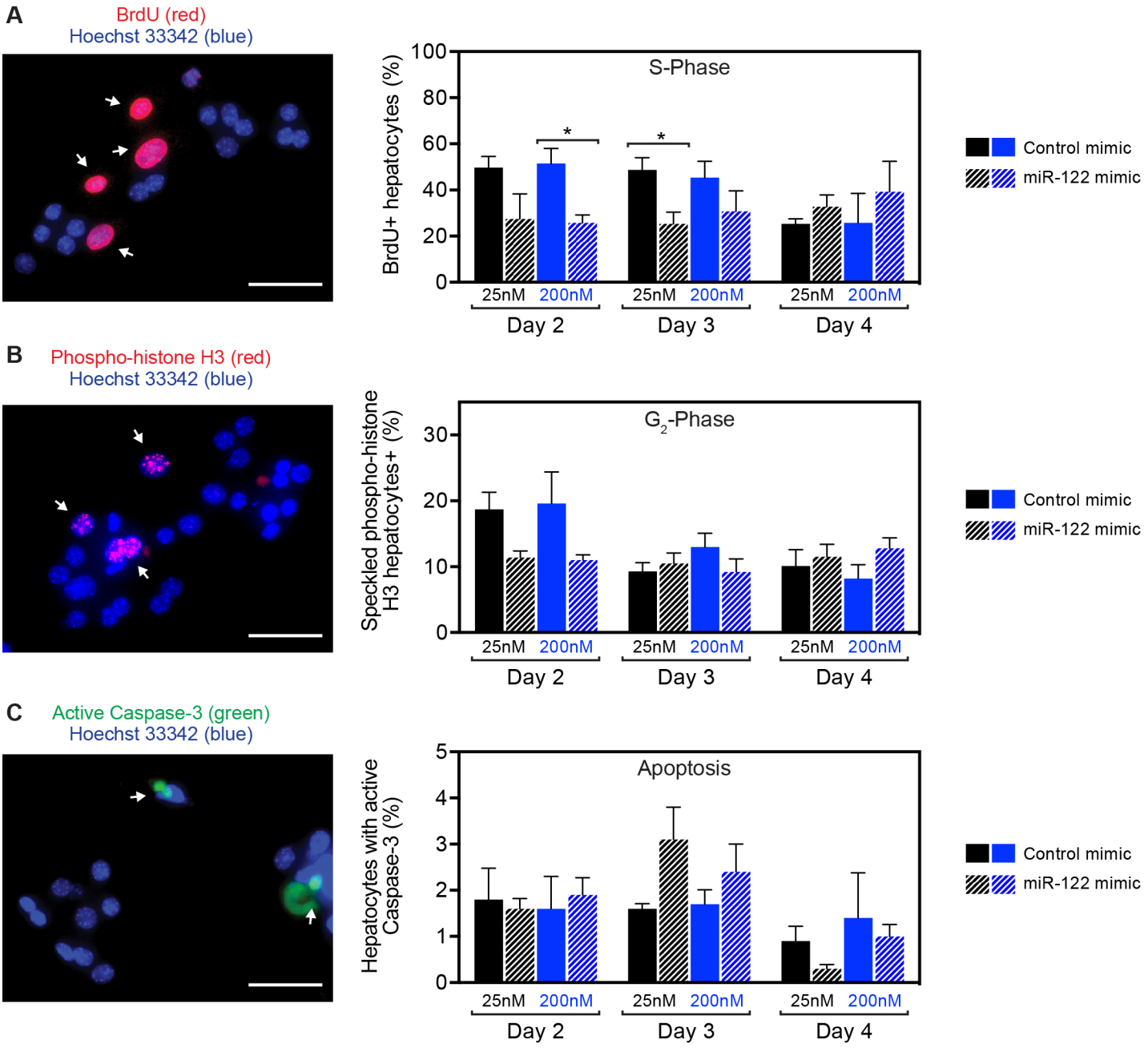

Supporting Fig. 5. Proliferation kinetics for diploid hepatocytes transfected with miR-122 mimic. Hepatocytes isolated from 14d-old WT C57BL/6 mice (described in Fig. 4A) were placed in culture on day 0 and transfected with 25 nM or 200 nM of miR-122 mimic or control mimic (n = 3). (A) Hepatocyte cultures were harvested on days 2-4 (following 24h BrdU pulse) and stained with Hoechst 33342 and an antibody for BrdU. A representative image is shown at day 2; arrows mark BrdU+ cells. The percentage of BrdU+ hepatocytes is reported. (B) Hepatocyte cultures were harvested on days 2-4 and stained with Hoechst 33342 and an antibody for phospho-histone H3 (PHH3). Speckled PHH3 nuclear staining indicates G_2-phase of the cell cycle. A representative image is shown at day 2; arrows mark cells with speckled staining. The percentage of hepatocytes positive for speckled PHH3 is reported. (C) Hepatocyte cultures were harvested on days 2-4 (following 30 min. incubation with NucView 488, a caspase-3 substrate that marks apoptotic nuclei) and subsequently stained with Hoechst 33342. The substrate is cleaved in the presence of active caspase 3, binds DNA and fluoresces green. A representative image is shown at day 2; arrows indicate nuclei with active caspase-3. The percentage of hepatocytes with active caspase-3 (NucView 488+ and Hoechst 33342+) is reported. Graphs show mean ± SEM. * P = 0.03. Scale bars are 50 μm.

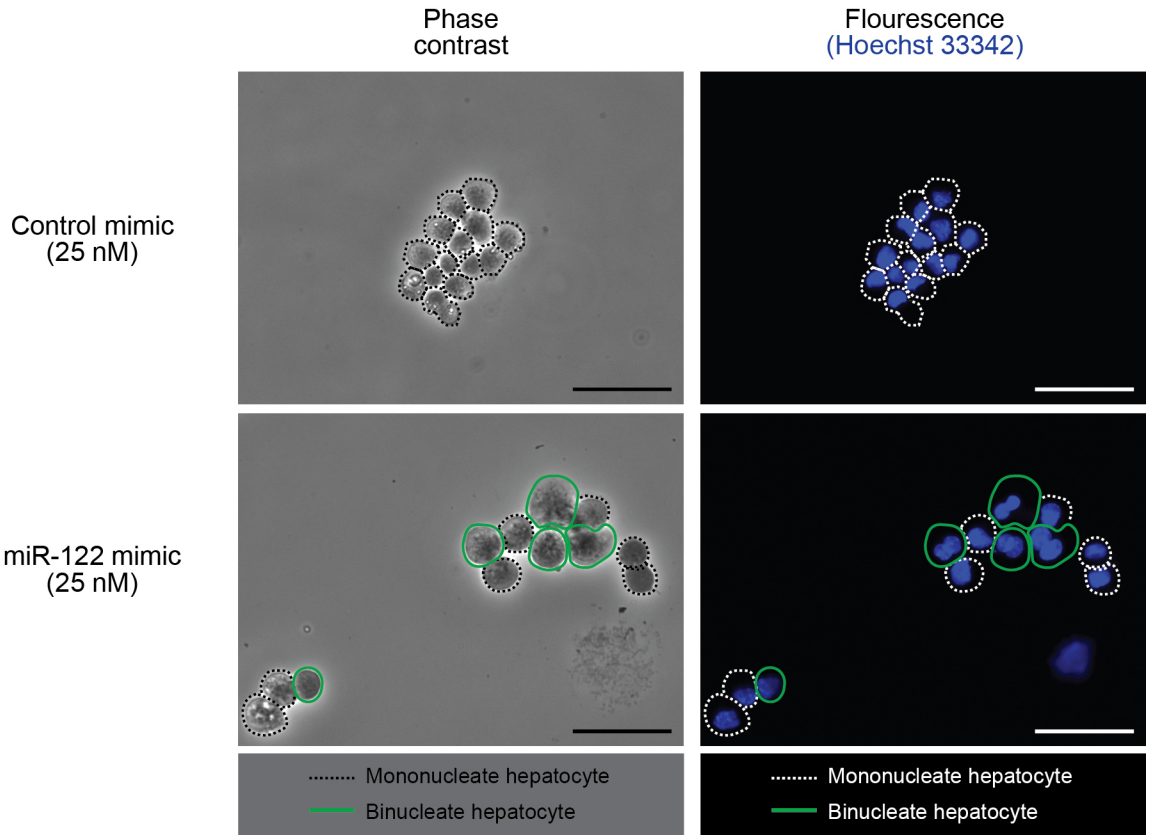

Supporting Fig. 6. Method for identification of mono- and binucleate hepatocytes in miR-122 mimic-transfected hepatocytes. Diploid WT hepatocytes from C57BL/6 mice were isolated, transfected with miR-122 mimic or control mimic (25 nM or 200 nM) and cultured for additional days, as indicated in Fig. 6A. Cultures were harvested on day 4 by trypsinization, cytospun onto slides and stained with Hoechst 33342. Individual cells were identified by phase contrast microscopy and nuclei (blue) were visualized by fluorescence microscopy. Dashed lines indicate mononucleate hepatocytes, and bold green lines mark binucleate hepatocytes. Representative images are shown. Fig. 4C shows the percentage of single hepatocytes with 2 nuclei. Scale bars are 50 μm.

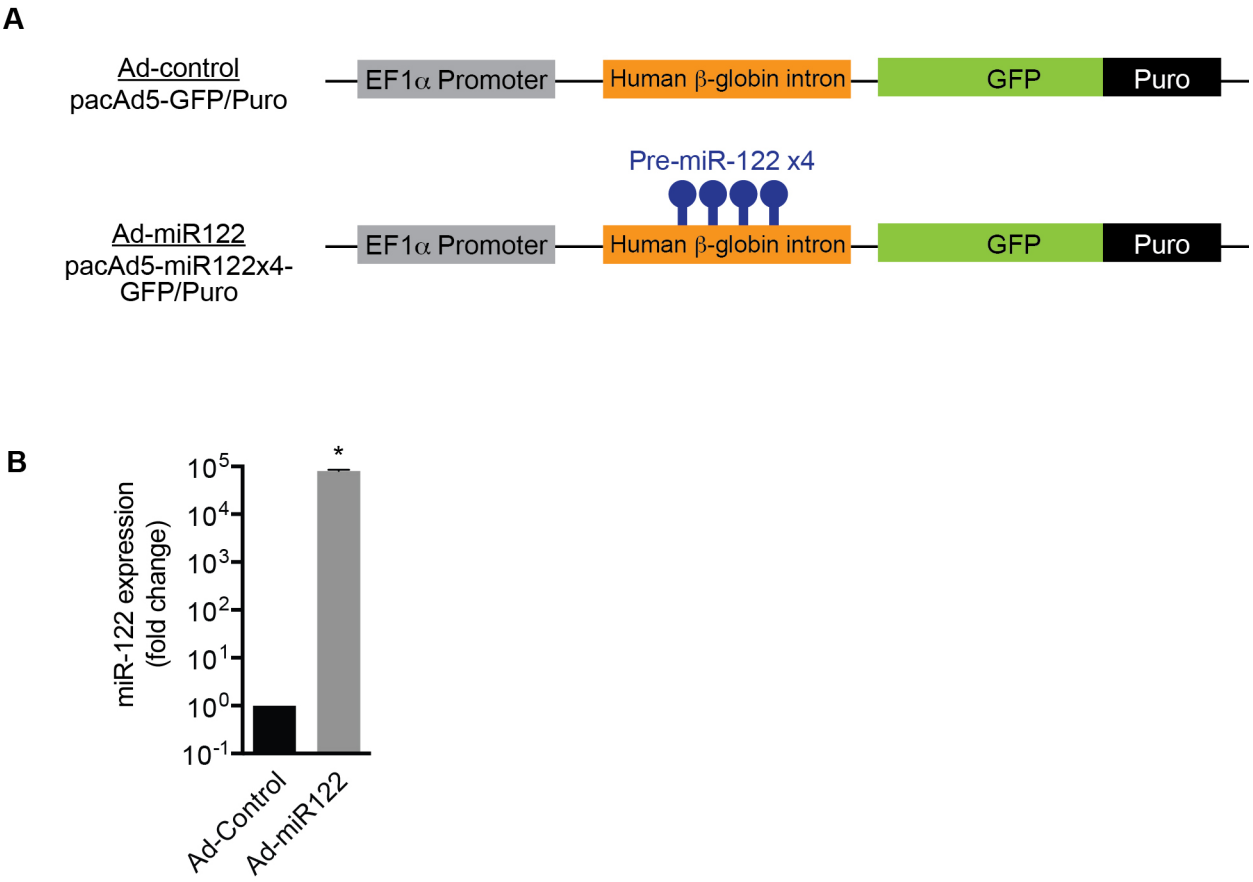

Supporting Fig. 7. miR-122 adenovirus induces miR-122 expression *in vitro*. (A) Four tandem copies of precursor miR-122 were cloned into the pacAd5-GFP/Puro plasmid from Cell Biolabs, Inc. Cartoons depict miR-122 adenovirus (Ad-miR122) and control adenovirus (Ad-control). (B) Hepatocytes isolated from 2.5mo-old *Mir122*-KO mice (n = 3) were placed in culture on day 0, infected with 0.6 x 10^9 viral particles of Ad-control or Ad-miR122 on day 1 and harvested on day 6. miR-122 expression, measured by qRT-PCR, was induced 80,000-fold in hepatocytes infected with Ad-miR122. Expression was normalized to RNU6b. * P = 0.00007. Graph shows mean ± SEM.

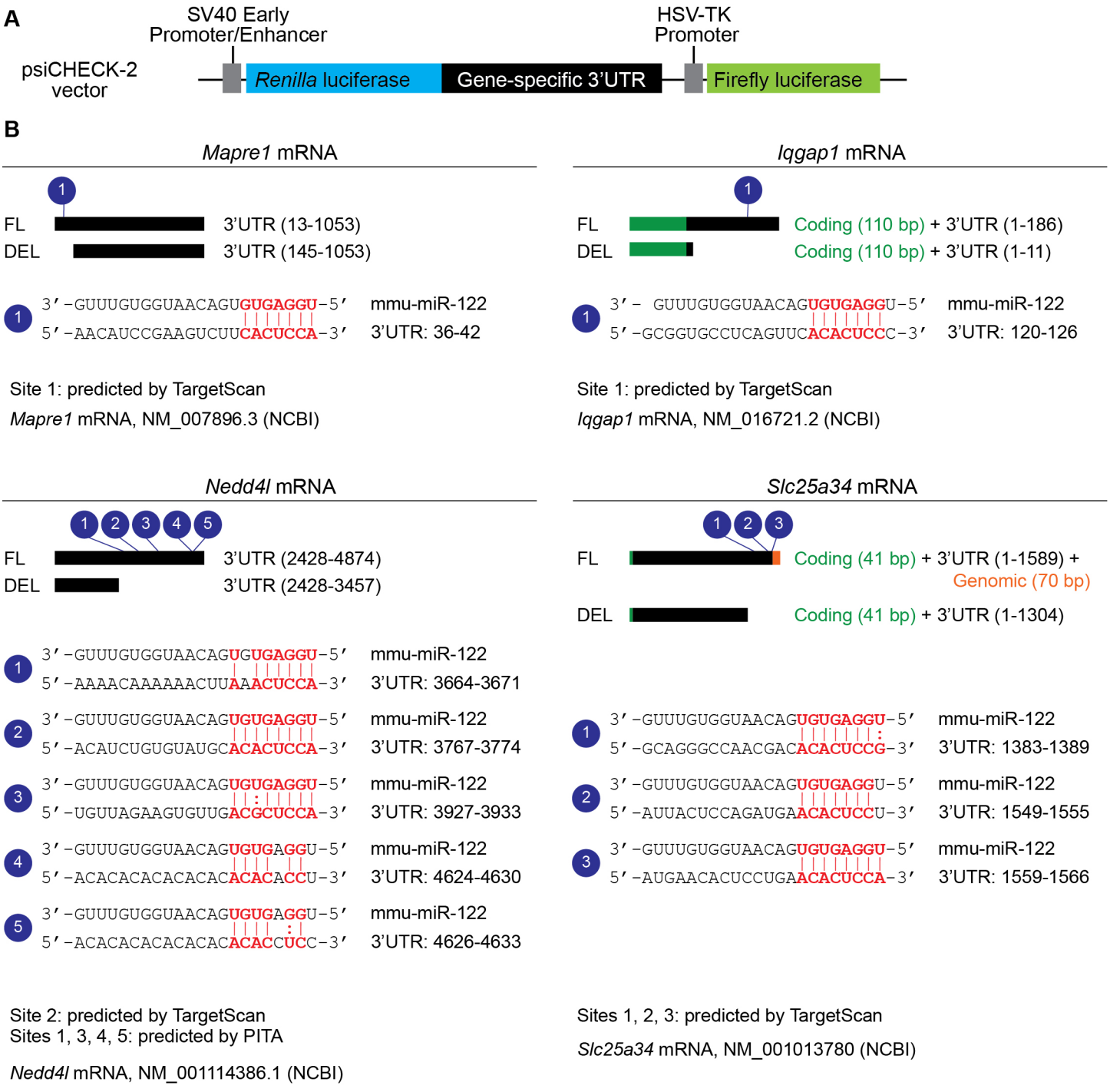

Supporting Fig. 8. miR-122 seed sequences in the 3'UTR of candidate genes. (A) Cartoon of the psiCHECK-2 plasmid detailing the insertion site for candidate 3'UTR that is adjacent to *Renilla* luciferase and independent of firefly luciferase. (B) *Mapre1, Iqgap1, Nedd4l* and *Slc25a34* are predicted to have miR-122 seed match sequences in their 3'UTR. *Mapre1* and *Iqgap1* are predicted to have a single seed match sequence, whereas *Nedd4l* and *Slc25a34* are predicted to have 5 and 3 sites, respectively. The location of each predicted miR-122 seed sequence within the 3'UTR is indicated graphically (blue circles); moreover, specific miRNA:mRNA binding sites are listed. Red letters depict sites of predicted pairing (straight lines indicate Watson-Crick pairing and colons indicate GU wobble base pairing). The algorithm used to identify predicted binding sites (TargetScan or PITA) is indicated. For each gene, the full-length (FL) construct contains the indicated the binding site(s), and the deleted (DEL) construct lacks the predicted binding sites(s).

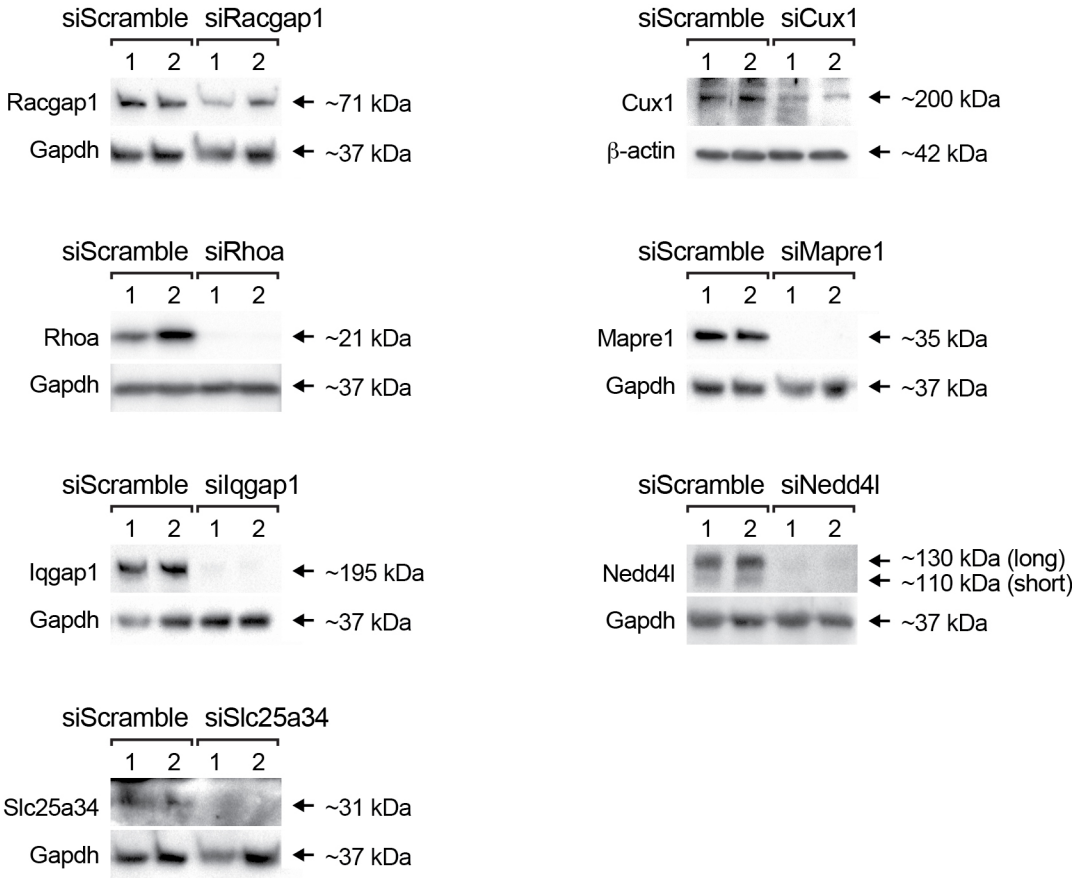

Supporting Fig. 9. Target proteins are down-regulated in hepatocytes transfected with target-specific siRNAs. Hepatocytes from 14-15d-old WT C57BL/6 mice were transfected with scrambled siRNA or siRNAs to *Racgap1, Cux1, Rhoa, Mapre1, Iqgap1, Nedd4l* or *Slc25a34,* as described in Fig. 6A. On day 4, western blotting revealed reduced protein expression in samples transfected with target-specific siRNAs (*n* = 2) compared to samples transfected with scrambled siRNA (*n* = 2). Gapdh served as a loading control for Racgap1, Rhoa, Mapre1, Iqgap1, Nedd4l and Slc25a34. β-actin served as a loading control for Cux1.

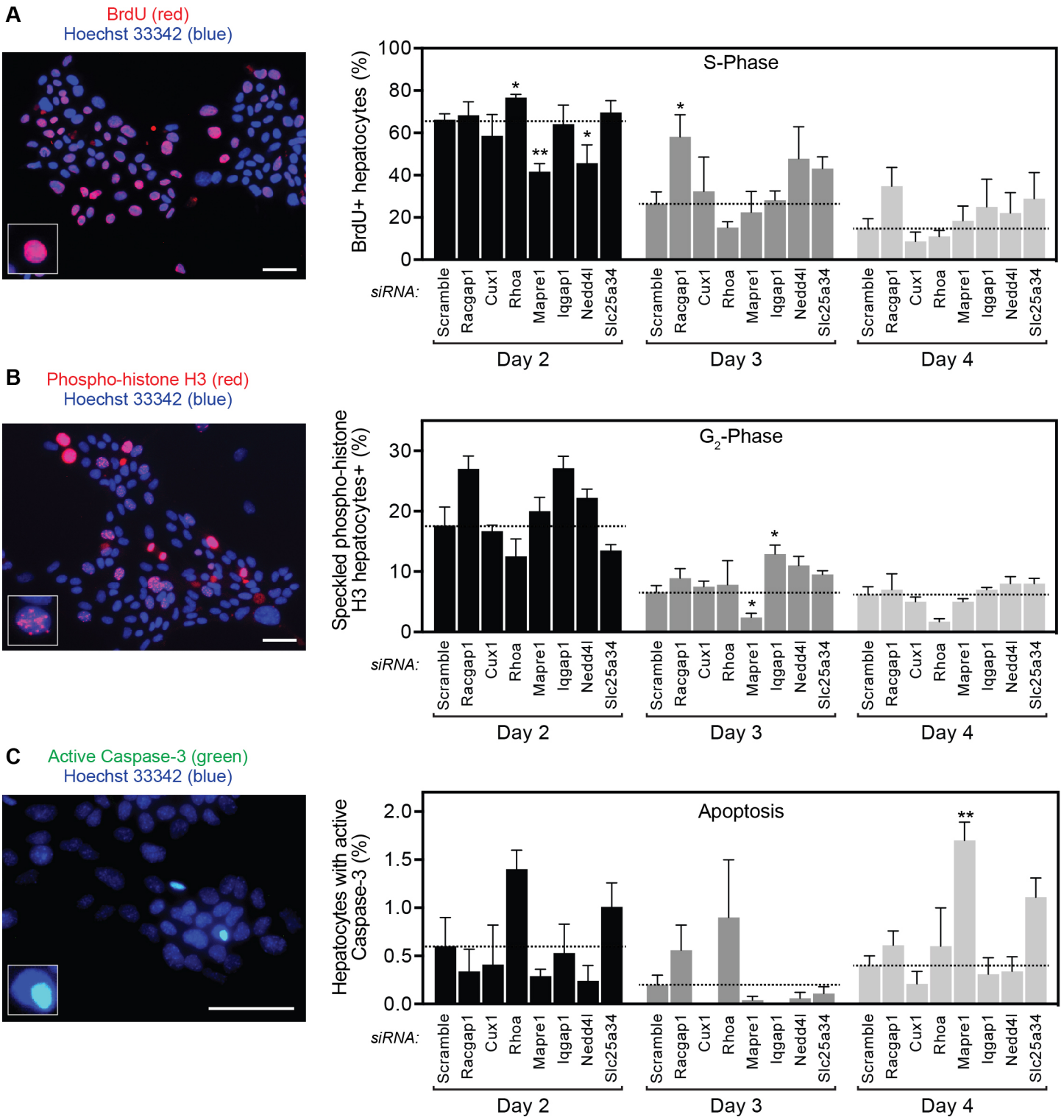

Supporting Fig. 10. Proliferation kinetics for diploid hepatocytes depleted of miR-122 target genes. Hepatocytes isolated from 14-15d-old WT C57BL/6 mice (described in Fig. 6A) were placed in culture on day 0 and transfected with 40 nM scrambled siRNA or siRNAs to *Racgap1, Cux1, Rhoa, Mapre1, Iqgap1, Nedd4l* or *Slc25a34* (*n* = 3-6). (A) Hepatocyte cultures were harvested on days 2-4 (following 24h BrdU pulse) and stained with Hoechst 33342 and an antibody for BrdU. A representative image is shown at day 3; the inset is a magnified image of a BrdU+ cell. The percentage of BrdU+ hepatocytes is reported. (B) Hepatocyte cultures were harvested on days 2-4 and stained with Hoechst 33342 and an

antibody for phospho-histone H3 (PHH3). Speckled PHH3 nuclear staining indicates G_2-phase of the cell cycle. A representative image is shown at day 3; the inset is a magnified nucleus with speckled staining. The percentage of hepatocytes positive for speckled PHH3 is reported. (C) Hepatocyte cultures were harvested on days 2-4 (following 30 min. incubation with NucView 488, a caspase-3 substrate that marks apoptotic nuclei) and subsequently stained with Hoechst 33342. The substrate is cleaved in the presence of active caspase 3, binds DNA and fluoresces green. A representative image is shown at day 4; the inset is a magnified image of a positive nucleus. The percentage of hepatocytes with active caspase-3 (NucView 488+ and Hoechst 33342+) is reported. Graphs show mean ± SEM. Dashed lines indicate values for hepatocytes transfected with siScramble at each time point. * $P < 0.05$, ** $P < 0.002$, compared to siScramble. Scale bars are 50 μm.

Overall, proliferation by target-depleted hepatocytes varied day-by-day, but there was a significant trend toward decreased proliferation by cells depleted of *Cux1* (i.e., PHH3-day 2), *Mapre1* (i.e., BrdU-day 2, PHH3-day 3) and *Slc25a34* (i.e., PHH3-day 2). The percentage of cells undergoing apoptosis was <2%, indicating that depletion of each gene minimally affected cell death.

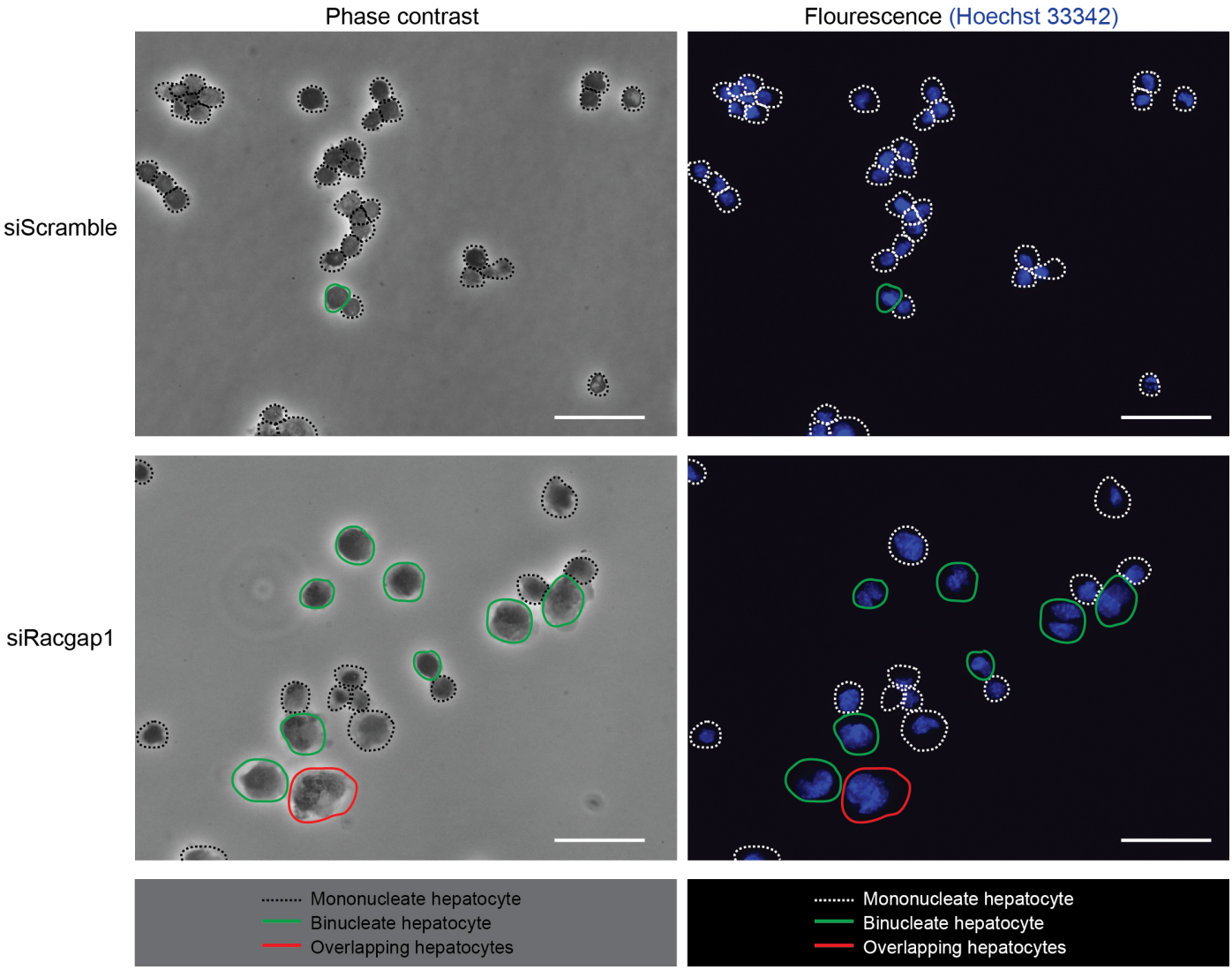

Supporting Fig. 11. Method for identification of mono- and binucleate hepatocytes in siRNA-transfected hepatocytes. Diploid WT hepatocytes from C57BL/6 mice were isolated, transfected with siRNAs to target genes (*Racgap1, Cux1, Rhoa, Mapre1, Iqgap1, Nedd4l* and *Slc25a34*) and cultured for additional days, as indicated in Fig. 6A. Cultures were harvested on day 4 by trypsinization, cytospun onto slides and stained with Hoechst 33342. Individual cells were identified by phase contrast microscopy and nuclei (blue) were visualized by fluorescence microscopy. Dashed lines indicate mononucleate hepatocytes, and bold green lines mark binucleate hepatocytes. The solid red line marks a cluster of overlapping hepatocytes with 2 or more adjacent cells with poorly defined borders; these types of clusters were not scored. Representative images are shown. Diploid hepatocytes transfected with scrambled siRNA were predominantly mononucleate: a single binucleate cell is shown. In contrast, hepatocytes transfected with *Racgap1* siRNA generated multiple binucleate cells. Fig. 6D shows the percentage of single hepatocytes with 2 nuclei. Scale bars are 50 µm.